

Research Article

Influence of Walnut Shell Dopant on the Properties of Walnut Doped-PbS Thin Film Crystals Grown by Sol-gel Technique

Achilefu Blessing Chinyere¹, Okpala Uchechukwu Vincent², Nwori Augustine Nwode^{3*}

^{1,2,3}Dept. of Industrial Physics, Chukwuemeka Odumegwu Ojukwu University Uli, Anambra State, Nigeria

*Corresponding Author: austine2010forreal@yahoo.com

Received: 23/Feb/2024; Accepted: 25/Mar/2024; Published: 30/Apr/2024

Abstract— Thin film crystals of walnut doped-lead sulfide (walnut/PbS) have been successfully grown using the Sol-gel method and characterized for device applications in this report. Lead nitrate ($\text{Pb}(\text{NO}_3)_2$), thiourea, sodium silicate, tartaric acid [$\text{HOOC}(\text{CHOH})_2\text{COOH}$] and locally prepared grinded walnut back cover/shell were the precursors used for the synthesis of the crystal films. The structural and optical properties of the films were investigated via x-ray diffraction (XRD) and spectrophotometry techniques respectively while the FT-IR technique was used to determine the functional group compositions of the films. The results of the characterisations indicated that the optical properties of the films like the absorbance, reflectance and refractive are quite high and are influenced by walnut doping. The bandgap energy of the films is in the range of 1.51 eV to 1.92 eV., which is strategic for many electronic and optoelectronic device applications. The XRD analysis showed that the grown crystals are crystalline in nature and crystal parameters such as grain size are 11.87 nm, 13.08 nm, 14.75 nm and 36.77 nm for un-doped, 1 drop, 2 drops, 3 drops walnut-doped PbS films respectively. The dislocation density of the films decreased as the number of walnut dopants drops increased which suggest improvement in the structure of the films. The FT-IR results indicated that the grown crystals composed mostly the N-H, O-H (alcohol stretching) and C-H (alkane stretching bond) functional groups. These properties exhibited by the grown films position them for many opto-electronics applications including infrared detectors, solar cells, photodetectors devices, waveguide and optical fiber device applications.

Keywords— Lead-sulfide, Bandgap, Walnut, Detectors, Solar Cells, Sol-gel, Doping.

1. Introduction

Materials that have narrow bandgap energy values have been found to be of great interests for many technological applications due to their peculiar characteristics. These characteristics stemmed from their small bandgap energy values, fast carrier mobility, high absorption capability and easy tunability of their structures. Basically, semiconductor materials that have bandgap energy of at most 2.3 eV can be described as narrow bandgap semiconductors (NBGs) and typical examples are group IV, III-V, IV-VI, and some IIB-VIA compounds, [1]. Most semiconductor materials obtainable from these groups of semiconductor compounds are Ge, InAs, InSb, GaSb, PbS, PbTe, and some ternary compounds such as InGaAs, HgCdTe from the groups, [2]. These materials have found good applications in fabrications of devices such as; Infrared detectors, laser, flash memory devices, thermal imaging cameras, photo-electromagnetic detectors, photodiodes, transistors, High speed electronics and solar cell, LEDs, Ohmic contact, electro-optic and host of other optoelectronic device applications, [3, 4]. The semiconductor chalcogenides of IV-VI materials/ thin films

such as PbS, PbTe, PbSe etc., have been identified to exhibit unique properties for tunable device applications. Specifically, PbS materials have been known to have bandgap energy in the range of 0.37–0.41 eV and large excitonic Bohr radius of about 18 nm at room temperature, [5, 6]. The relatively large exciton Bohr radius of PbS is strategic in the sense that comparable size reduction to the nano-meter scale regime can be easily achieved in the crystal structures of PbS thin films and this phenomenon known as “quantum confinement effect” has been one of the keys to exploring the various applications of PbS materials in nano or thin film forms, [7, 8]. Basically, PbS has been found very useful in fabrications of devices for photodetectors, solar cells, infrared (IR) detector, solid state lasers, biosensors, deep tissue imaging, etc., [9]. In solar energy application in particular, it has been reported that PbS-based solar cells combined with silicon solar cells can improve performance due to the additional absorption in the infrared range coming from the PbS base, [10, 11]. Doping of PbS thin film semiconductors with different materials and fabricate using several deposition methods at different conditions have been found to alter the

various properties of the PbS materials for different device applications, [12, 14].

2. Related Work

In this respect, the influence of Cu-doping on the morphological and electrical properties of PbS thin films have been reported by, [15]. The authors reported that there is decrease in the surface roughness and grain size of the films as the concentration of Cu^{2+} increased from 0.5 to 2.0 at% while the electrical conductivity was found to increase with Cu^{2+} doping as from 1.0 to 1.5 at%. The authors inferred that Cu doping can be an effective strategy to tuning the electrical properties of PbS thin films for development of suitable optically active materials for photovoltaics applications. The structural and electrical properties of PbS thin films doped with Cr^{3+} ions using chemical deposition method has also been reported by, [16]. The authors observed high variations in the structural properties of the films such as lattice parameters, strains, and degree of texturing and the band gap energy of doped PbS. The photoelectric and electrical properties showed an extremum and the most profound changes were observed for the film deposited with 0.016 M chromium source. Study on the optical, electrical, structural and morphological properties of lead manganese sulphide (PbMnS) thin film semiconductors for possible device applications has been reported by, [17]. The band gap energy of the PbS film was found to be tuned to the order of 1.9 eV to 2.0 eV as a result of Mn doping and tends to remain constant as concentration of Mn^{2+} increased. The electrical resistivity and conductivity of the films were found to be dependent on the concentration of Mn^{2+} and film thickness. The authors concluded that the observed properties exhibited by the films of PbMnS made them good materials for many optoelectronic and electronic applications such as solar cell, light emitting diode (LED), photodetector etc. A comprehensive study of the effects of Mn doping on the electronic density of states of PbS quantum dots (QDs) has also been reported by, [18]. It was found that the Mn doping caused variations in broadening of the electronic bandgap in the PbS QDs and sp-d hybridization between the PbS host material and Mn dopants was believed to be responsible for the bandgap broadening in the deposited material. The study on the effect of deposition voltage variation on the optical properties of PbMnS thin films deposited by electrodeposition method to determine the optimum voltage for device application has been reported by, [19]. The authors reported that the optical bandgap energy of the deposited PbMnS thin films is in the range of 1.5 eV to 1.9 eV and Urbach energy showed increasing trend as the deposition voltage increased. They concluded that the bandgap energy of the films is blue-shifted and based on the Urbach energy variation, the optimum deposition voltage for the films is at lower voltage in the order of 1.80-2.20 V. The properties of Ag-doped PbS nanoparticles for optoelectronic applications have been reported by, [20]. It was discovered that Ag doping improved the electrical and dielectric properties of PbS nanoparticles and there exist enhanced photodetector figures of merit compared to the un-doped PbS nanoparticles. The optical band gap energy was found to increase to the range of

1.95–2.51 eV as Ag doping concentration increased. However, there was quenching in photoluminescence (PL) intensity with increase in Ag doping concentration and that was attributed to the charge transfer between Ag and PbS. The physicochemical and electrical characteristics of lead sulphide (PbS) nanoparticles (NPs) doped with manganese (Mn) for electronic device applications has been studied and reported by, [21]. The bandgap energy of the doped samples was found to decreased from 1.48 to 1.42 eV by increasing the concentration of Mn ion source compared to the pure PbS nanoparticles. The electrical properties such as electrical resistivity and conductivity were found to be enhanced without any structural distortions. The authors concluded that pure PbS and Mn-doped PbS nanoparticles are suitable for electronic devices operated at low temperatures. The structure and photoelectrochemical activity of Cr-doped PbS thin films grown by chemical bath deposition have been studied and reported by, [22]. The study showed that Cr incorporation decreased the average crystallite size of PbS from 59.97 to 37.59 nm, average sizes of nanoclusters decreased from 73 to 41 nm while the micro-strain and dislocation density of the doped samples were found to increase. The study also showed that the optimum values for incident photon-to-current efficiency and applied bias photon-to-current efficiency were 13.5% and 1.44% at 0.68 V and 390 nm wavelength respectively. The properties of Ba-doped PbS thin films prepared by the SILAR method have also been reported by, [23]. The author stated that Ba-doping influenced the structural and optical properties of the PbS thin films. The crystallite size, optical bandgap energy and transmittance of the doped films were found to increase with increase in Ba doping. Al doped PbS thin films for heterostructure solar cell device fabrication using nebulizer spray pyrolysis technique is been reported by, [24]. It was reported that bandgap values of PbS was shifted from 1.54 eV to 1.66 eV on increasing Al doping concentration while the electrical resistivity was found decreased from 3.08×10^3 to $1.63 \times 10^3 \Omega\text{cm}$ as Al doping increased. The solar cell efficiency of the film fabricated with 6% of Al doping was found to be about 0.44%. In this paper, we report the properties of PbS thin film crystals doped with local material (grinded walnut shells) for the first time using the sol-gel method to determine the influenced of walnut dopant on the properties of the material for device applications. The choice of the walnut shell as the dopant is attributable to the remarkable characteristics of the material for different uses and applications, [25]

3. Theory/Calculations

The various properties of the un-doped and walnut doped PbS thin films studied include the following:

Transmittance: this property is calculated based on the measured absorbance values of the thin films using Beer-Lambert relation as given by [26, 27].

$$T = 10^{-A} \quad (1)$$

Where A is the absorbance.

Reflectance: this was evaluated using the relation given by [28].

$$R = 1 - \left(\frac{e}{10}\right)^{A/2} \quad (2)$$

Extinction coefficient: this property determines the degree a material can with stand light intensity before actual extinction from the material. It can be calculated using the equation as given by [29].

$$k = \frac{\alpha\lambda}{4\pi} \quad (3)$$

Where α is the absorption coefficient given by [30].

$$\alpha = \frac{A}{\lambda} \quad (4)$$

Refractive index: the refractive index of the grown thin film crystals was calculated using the relation given by, [31].

$$n = \frac{1+R^{0.5}}{1-R^{0.5}} \quad (5)$$

Bandgap energy: this other property is a very important property of thin film material and can be estimated in this work using Tauc formula by plotting $(\alpha h\nu)^2$ as a function of photon energy [32, 33].

$$(\alpha h\nu)^2 = A(h\nu - E_g) \quad (6)$$

Crystallite size and dislocation density and micro-strain: these properties of the grown material were estimated using the Williamson-Hall (W-H) plots and Wilson relations. In the W-H scatter plot, $\beta_{hkl}\cos\theta$ is plotted as a function of $4\sin\theta$ and a linear fitting gives intercept (z) on the $\beta_{hkl}\cos\theta$ axis as $k\lambda/D_{hkl}$ while the slope represents the micro-strain (ϵ) of the material. The W-H and Wilson relations are as provided by [34, 35].

$$\beta_{hkl}\cos\theta = \frac{k\lambda}{D_{hkl}} + 4\epsilon\sin\theta \quad (7)$$

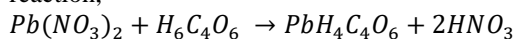
$$\delta = \frac{1}{D^2} \quad (8)$$

4. Experimental Method/Procedure

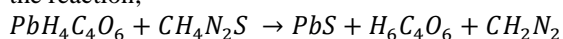
Materials used in this work were 5 ml measuring cylinder, magnetic stirrer with hot plate and magnetic bead, electric oven and Whatman filter paper (110 mm) thick, digital weighing balance and 100 ml glass beakers. The reagents used include; lead nitrate ($Pb(NO_3)_2$), thiourea, sodium silicate, tartaric acid [$HOOC(CHOH)_2COOH$] and locally prepared grinded walnut back cover (walnut shell). Sol-gel method was utilized in the preparation of the thin film crystal samples.

4.1 Experimental details

The crystals of lead sulphide (PbS) thin films were grown by titrating different quantities of sodium silicate solution (pH - 11.0) in 100 ml beakers, with appropriate quantities of 1 M tartaric acid [$HOOC(CHOH)_2COOH$], until gel was formed. The set gels were added with 20 ml, of 1 M lead nitrate $Pb(NO_3)_2$ solution to form lead tartanate as shown in the reaction,



The precipitation of lead-tartanate was allowed for two weeks to be completed. Thereafter, 20 ml, 25 ml, 30 ml and 35 ml of 1 M thiourea were added to obtain lead sulfide according to the reaction;



Finally, different pipette drops of locally produced impurity (solution of grinded walnut shells), were added as dopant to

dope the PbS films as shown in Table 1 to obtain the walnut doped PbS (walnut/PbS) thin film crystals.

Table 1: The concentration of the precursors used for the growth of undoped and walnut/PbS crystals

Samples	Quantity of Na_2SiO_3 (ml)	Quantity of tartaric acid (ml)	Quantity of $Pb(NO_3)_2$ (ml)	Quantity. of thiourea (ml)	Quantity. of walnut solution
E1	20.0	12	20	20.0	0 pipette drop
E2	25.0	14	20	25.0	1 pipette drop
E3	30.0	16	20	30.0	2 pipettes drop
E4	35.0	18	20	35.0	3pipettes drop

4.2 Sample characterizations

The grown thin film crystals of PbS and walnut doped PbS were characterized using x-ray diffraction (XRD), UV-VIS spectrophotometry and Fourier transformed infrared spectroscopy (FT-IR) techniques to determine their structural, optical and compositional properties for suitable device applications. The analysis of the results of these characterisations are displayed in figures 1 to 9.

5. Results and Discussion

5.1 Optical properties of the grown crystals

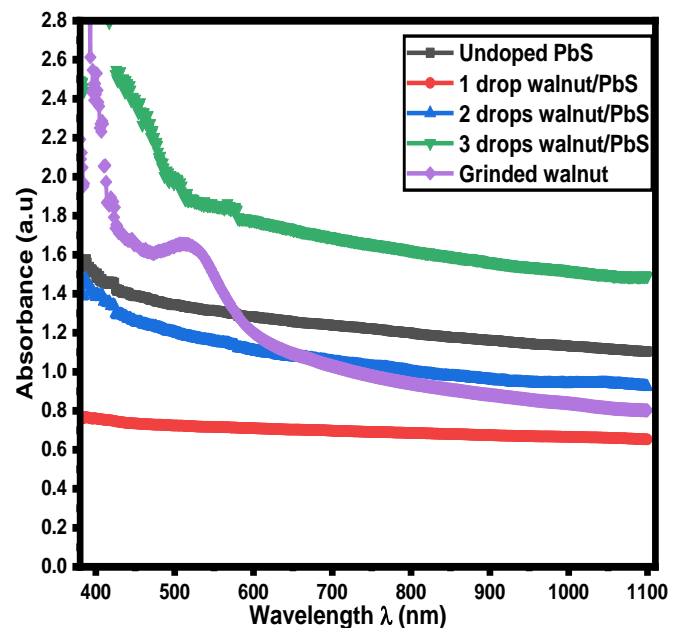


Figure 1: Graph of Absorbance against wavelength for the undoped and walnut/PbS crystals.

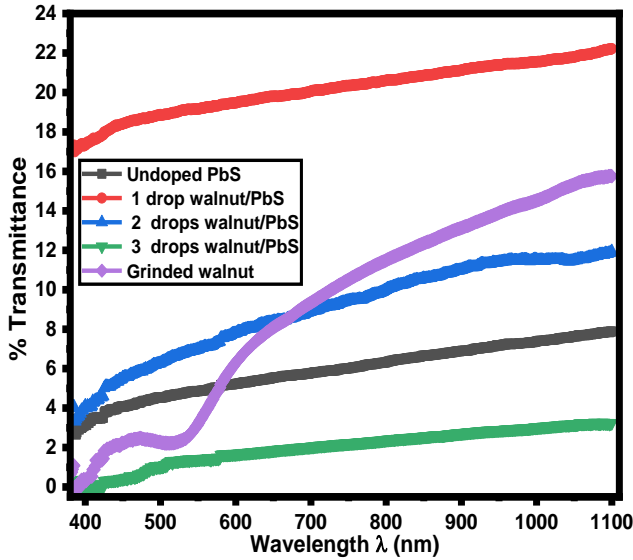


Figure 2: Graph of Percentage Transmittance against wavelength for the undoped and walnut/PbS crystals.

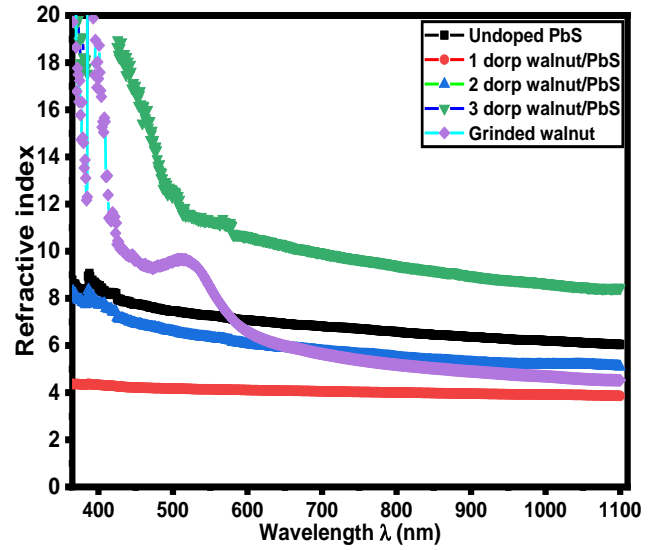


Figure 5: Graph of Refractive index against wavelength for the undoped and walnut/PbS crystals

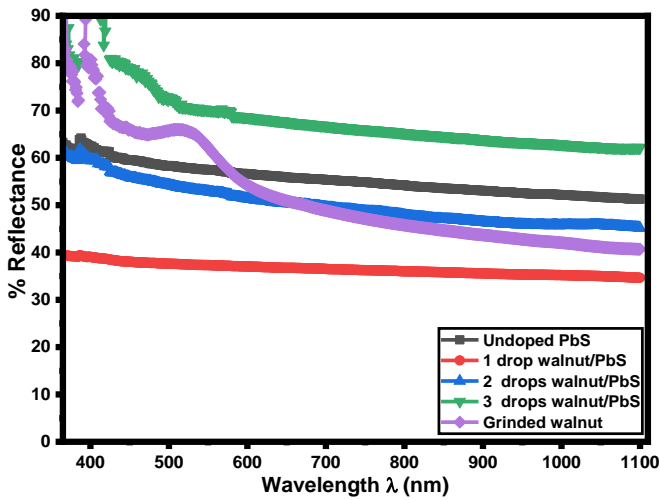


Figure 3: Graph of Percentage Reflectance against wavelength for the un-doped and walnut/PbS crystals.

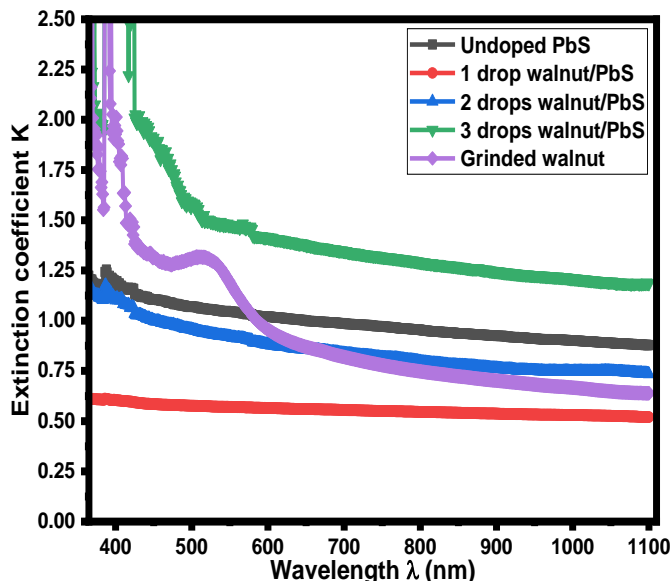


Figure 4: Graph of Extinction coefficient against wavelength for the undoped and walnut/PbS crystals.

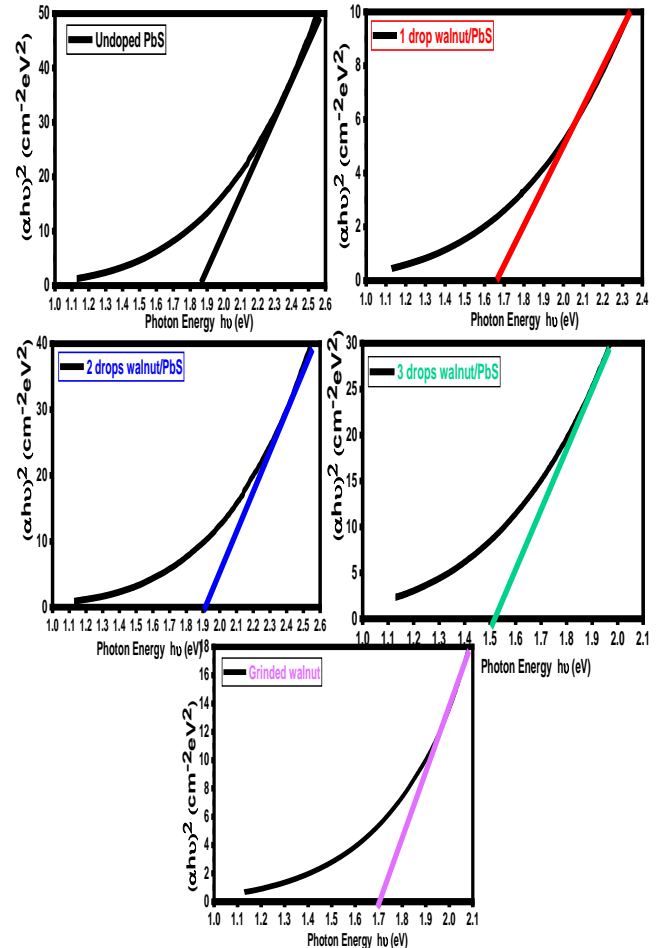


Figure 6: Plots of $(\alpha h\nu)^2$ against photon energy for undoped and walnut/PbS crystals.

5.2 Structural Properties

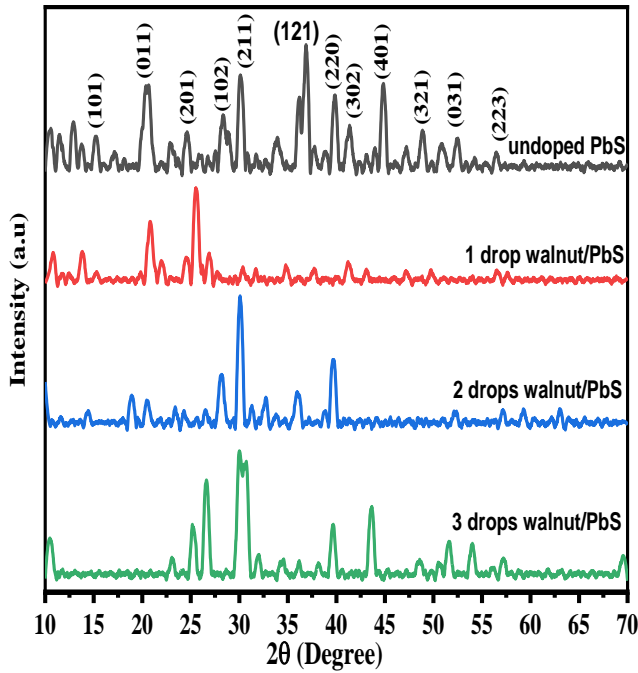


Figure 7: XRD patterns of the grown walnut/PbS crystals.

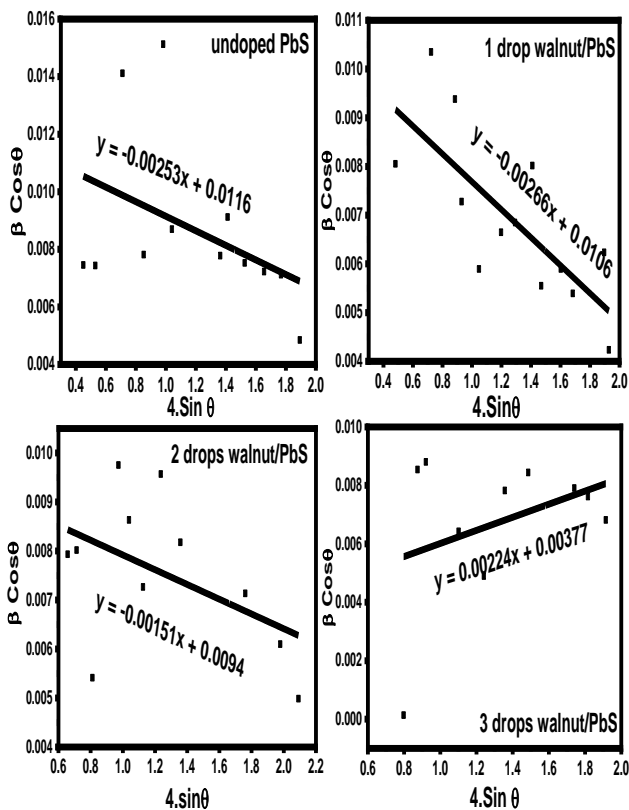


Figure 8: W-H plots of the deposited thin films of undoped and walnut/PbS crystals

5.3 Fourier transform infrared spectroscopy analysis results.

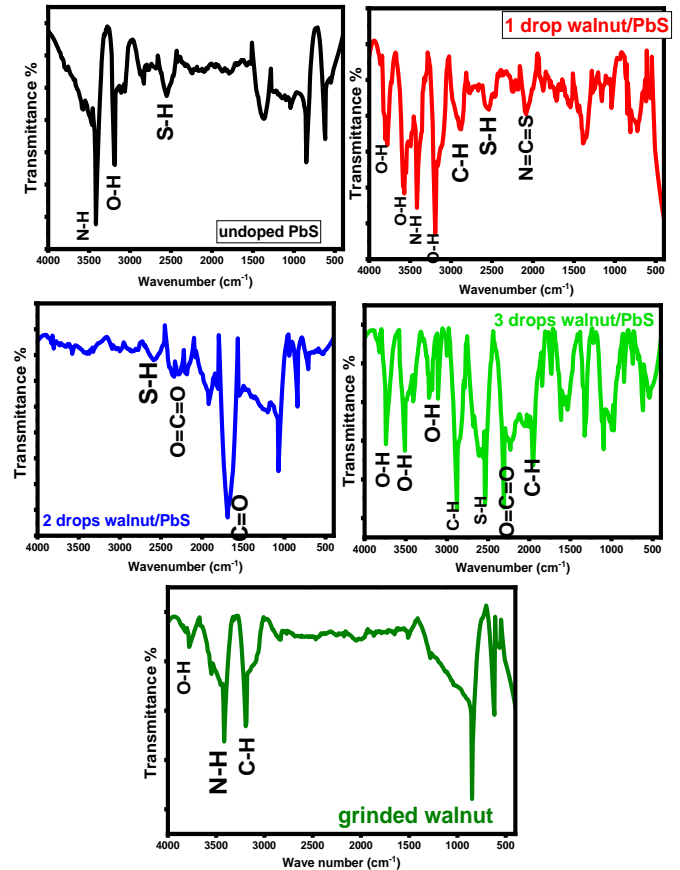


Figure 9: Plot of FTIR profiles of the grown undoped and walnut/PbS crystals.

Discussion

Figure 1 is the graph of the absorbance property of the undoped and walnut/PbS thin film crystals against wavelength. The figure showed that the grown crystals have high absorbance values in the near visible (VIS) region and decreased with increase in wavelength, towards the infrared region. The absorbance of the grinded walnut followed the same path. These results indicate that grinded walnut used as dopant can increased the absorbance of PbS materials and the obtained results are good for optoelectronic applications such as solar cell devices for solar energy harnessing. In figure 2, the graph of transmittance against wavelength for the grown crystals is displayed. The figure indicated that the transmittance of the grown crystals increased with an increase in wavelength which suggest higher percentage transmittance in the infra-red (IR) region. This made the samples good materials for photovoltaic cells and poultry house coating applications, [36]. Figure 3 is the graph of percentage reflectance of the un-doped and walnut/PbS films. The grown crystal films exhibited high reflectance of the order 70-80 % for the crystal doped with 3 drops of walnut solution, 60-65 % for un-doped and 2 drops walnut/PbS, and decreased towards the infrared region. The sample 1 drop walnut/PbS has reflectance of 40 % in the near visible region, decreased a bit at the visible region and remained steady towards the infrared region. The grinded walnut sample has a percentage reflectance in the range 70-75% in the VIS region and decreased towards the infrared region. The high percentage

reflectance exhibited by the grown crystals of the undoped and walnut/PbS make them good materials for eye glass coatings. The graph of extinction coefficient of the grown crystals as a function of wavelength is displayed in figure 4. This property indicates how strongly a material absorb light at a given wavelength and the graph showed that the extinction coefficient is higher at the VIS and decreased towards the infrared region; except for the film 1 drop walnut/PbS that remained steady towards the infrared. The crystal doped with 3 drops of walnut solution has the highest extinction coefficient. The graph of refractive index against wavelength is shown in figure 5 to determine the refractive index behaviors of the films at different wavelength range. From the figure, it was observed that the grown film crystals exhibit high refractive index values in the VIS region. The film grown with 2 drops walnut has the highest value in the range 8-19 while the film grown with 1 drop walnut dopant has the lowest value of 4.0 throughout the VIS and NIR regions. The figure also showed that the walnut dopant has influence on the refractive index of the films and the obtained results are favorable for waveguide and optical fiber device applications. Figure 6 showed the plots of $(\alpha h\nu)^2$ as a function of photon energy for determination of the optical bandgap energy of the grown crystals of undoped and walnut/PbS. From the plots, the bandgap energies of the samples were extrapolated on the photon energy axes at absorption edge at which $(\alpha h\nu)^2$ equals to zero. The values obtained are 1.86 eV for undoped PbS, 1.66 eV for 1 drop walnut/PbS, 1.92 eV for 2 drops walnut/PbS, 1.51 eV for 3 drops walnut/PbS and 1.70 eV for the grinded walnut sample. These results showed that grinded walnut dopant has effect on the bandgap energy of PbS crystals. The bandgap energy values ranged from 1.51 eV-1.92 eV., implying that the grown crystals have wide bandgap and can be used in solar energy technology, high temperature and power devices, high frequency and optoelectronic devices, [37]. Figure 7 is the plots of XRD patterns of the results of XRD analysis done on the grown crystal films of un-doped and walnut/PbS. From the figure, there exist sharp peaks in the XRD profiles which indicated that the grown crystals are crystalline. These peaks that occurred at various 2-theta positions are indexed to different crystal planes as depicted in the figure. The data from database of Qual X Software were used to match the XRD results of the grown crystals and the data for all the samples matched almost well with the standard JCPDS card no. 00-901-4778 for PbS (Anglesite) with Space Group - Pnma and Orthorhombic crystal structure. The Williamson-Hall (W-H) plots of the deposited thin film crystals are presented in figure 8. The figure showed negative slopes for undoped PbS, 1 drop, 2 drops and 3 drops doped PbS which suggest that the micro-strain is due to compression/shrinkage of lattice parameters of the deposited films, while the sample 3 drops walnut/PbS has a positive slope indicating strain may be due to expansion of lattice parameter at higher concentration of the dopant. The crystallite sizes of the films estimated from the W-H plots are 11.87 nm, 13.08 nm, 14.75 nm and 36.77 nm for un-doped, 1 drop, 2 drops, 3 drops doped PbS films respectively. The calculated values of dislocation densities of the films using Wilson relation based on the estimated values of crystallite sizes are $7.09 \times 10^{-3} \text{ nm}^{-2}$, $5.84 \times 10^{-3} \text{ nm}^{-2}$,

$4.59 \times 10^{-3} \text{ nm}^{-2}$ and $7.39 \times 10^{-4} \text{ nm}^{-2}$ respectively. The FT-IR spectra of the grown crystals of un-doped and walnut/PbS are presented in figure 9. The functional groups exhibited by the grown crystals were determined in the wavenumber range $1500 \text{ cm}^{-1} - 4000 \text{ cm}^{-1}$. The crystals exhibit various absorption sharp peaks within the functional group region as depicted in the figure. The sharp peaks around 3423 cm^{-1} and 3192 cm^{-1} signal the presence of N-H and O-H stretching while weak absorption peak at 2561 cm^{-1} indicated S-H stretching for undoped PbS crystal. The 1 drop walnut/pbS crystal showed sharp absorption peaks around 3802 cm^{-1} and 3587 cm^{-1} each corresponding to O-H (alcohol stretching), 3417 cm^{-1} correspond to N-H stretching while the peak at 2877 cm^{-1} indicates C-H (alkane stretching bond). There exist also absorption peaks 2537 cm^{-1} and 2082 cm^{-1} which signal S-H and N=C=S alkene double stretching in the crystal. The sample 3 drops walnut/PbS showed sharp peaks at 3751 cm^{-1} , 3500 cm^{-1} and 3208 cm^{-1} which were attributed to O-H (alcohol stretching). The C-H and S-H bonds are identified at wavenumbers 2873 cm^{-1} and 2538 cm^{-1} while O=C=O stretching occurred at 2287 cm^{-1} . The grinded walnut showed O-H at 3783 cm^{-1} , N-H stretching at 3427 cm^{-1} and C-H alkane stretching at 3190 cm^{-1} .

6. Conclusion and Future Scope

The properties of the deposited thin film crystals of un-doped and walnut/PbS studied in this work showed that the absorbance of the films is generally high and the obtained values are influenced by doping concentration. The film grown with 3 drops of walnut solution (3 drops walnut/PbS) has the highest value of absorbance in the range of 1.6-2.6 in the VIS and NIR regions. The film grown with 1 drop walnut solution has the lowest value of 0.75 throughout the VIS and NIR regions. The transmittance of the films is however low but increased with wavelength thus suggesting higher values in the infrared region of electromagnetic spectrum. The films exhibited high percentage reflectance as well as very high values of refractive index throughout the VIS and NIR regions and greatly influenced by doping of walnut solutions. The deposited thin films of PbS and walnut/PbS also have high extinction coefficient with the highest value in the range 1.25-2.00 exhibited by the sample 3 drops walnut/PbS. The bandgap energy of the films ranged from 1.51 eV to 1.92 eV., indicating that the grown crystals have range of bandgap values that can be used in solar energy technology, high temperature and power devices, high frequency and many other optoelectronic devices. The XRD analysis showed that the grown thin films have crystal structure and the crystallite sizes were found to be 11.87 nm, 13.08 nm, 14.75 nm and 36.77 nm for un-doped, 1 drop, 2 drops, 3 drops doped PbS films respectively while the dislocation densities are $7.09 \times 10^{-3} \text{ nm}^{-2}$, $5.84 \times 10^{-3} \text{ nm}^{-2}$, $4.59 \times 10^{-3} \text{ nm}^{-2}$ and $7.39 \times 10^{-4} \text{ nm}^{-2}$ respectively. The FT-IR results indicated that the grown crystals composed mostly of N-H, O-H (alcohol stretching) and C-H (alkane stretching bond) functional groups. The grinded walnut was specifically found to show absorption peaks at 3783 cm^{-1} , 3427 cm^{-1} and 3190 cm^{-1} which corresponded to O-H, N-H stretching and C-H alkane groups stretching. Following these properties exhibited by the grown

thin films of this nature, it can be asserted that the films are good candidates for many opto-electronics applications including infrared detectors, solar cells, photodetectors etc. The challenge to this research remains lack of grants from government agency and it is thus recommended that more properties of materials such as electrical, magnetic properties etc. be investigated to determine other potential areas of applications of the grown films of this nature.

Conflict of Interest

Authors declare that they do not have any conflict of interest.

Funding Source

No funding/grant was provided by any government agency to carry out this research work.

Authors' Contributions

The author Achilefu B. C. performed the experiment in closed supervision by the author Okpala U.V. for the preparation of the film samples subject to their characterizations and subsequent analysis. The author Okpala U.V. supervised and subsequently examined the whole work to completion. The author Nwori A.N. prepared the data analysis, the literature review and drafted the first manuscript subject to review by the second author. All authors reviewed and approved the final version of the manuscript as per the journal template for this publication.

Acknowledgements

The authors are grateful to the technologists - Udechukwu Ifeanyi and Obiechine Festus of the department of Industrial Physics Chukwuemeka Odumegwu Ojukwu University Uli Anambra State Nigeria for making the laboratory available to carry out the experimental preceding of this work. The team of scientists of Nano Science Laboratory, University of Nigeria Nsukka, Nigeria are also acknowledged for their helps in the characterizations of our samples.

References

- [1] S. An, H. Park, M. Kim, "Recent advances in single crystalline narrow band-gap semiconductor nanomembranes and their flexible optoelectronic device applications: Ge, GeSn, InGaAs, and 2D materials," *Journal of Materials Chemistry C*, Vol. **11**, pp. 2430–2448, 2023.
- [2] T. Safrani, T. A. Kumar, M. Klebanov, N. Arad-Vosk, R. Beach, A. Sa'Ar., ... Y. Golan, "Chemically deposited PbS thin film photo-conducting layers for optically addressed spatial light modulators," *Journal of Materials Chemistry C*, 2, No. **43**, pp. 9132-9140, 2014.
- [3] T. Tohidi, K. J. Ghaleh, A. Namdar, R. A. Ghaleh, "Comparative studies on the structural, morphological, optical, and electrical properties of nanocrystalline PbS thin films grown by chemical bath deposition using two different bath compositions," *Materials Science in Semiconductor Processing*, Vol. **25**, pp. 197–206, 2014.
- [4] L. Kungumadevi, R. Sathyamoorthy, "Structural, Electrical, and Optical Properties of PbTe Thin Films Prepared by Simple Flash Evaporation Method," *Advances in Condensed Matter Physics*, pp. 1-5, 2012
- [5] S. Thirumavalavan, K. Mani, S. Suresh, "Investigation on Structural, Optical, Morphological and Electrical Properties of Lead Sulphide (PbS) Thin Films," *Journal of Ovonic Research*, Vol. **11**, No. **3**, pp. 123 – 130, 2015.
- [6] B. A. Ezekoye, T. M. Emeakaroha, V. A. Ezekoye, K. O. Ighodalo, P. O. Offor, "Optical and structural properties of lead sulphide (PbS) thin films synthesized by chemical method." *International Journal of Physical Sciences*, Vol. **10**, No. **13**, pp. 385-390, 2015.
- [7] B. Abdallah, A. Ismail, H. Khashoua, W. Zetoun, "Effects of Deposition Time on the Morphology, Structure, and Optical Properties of PbS Thin Films Prepared by Chemical Bath Deposition" *Hindawi Journal of Nanomaterials*, pp. 1-8, 2018.
- [8] S. M. Ali, M.S. AlGarawi, S. Aldawood, S.A. Al Salman, S.S. AlGamdi, "Influence of gamma irradiation on the properties of PbS thin films," *Radiation Physics and Chemistry*, Vol. **171**, pp. 1-5, 2020.
- [9] A. B. Rohom, P. U. Londhe, P. R. Jadhav, G. R. Bhand, N. B. Chaur, "Studies on chemically synthesized PbS thin films for IR detector application", *Journal of Materials Science: Materials in Electronics*, Vol. **28**, pp. 17107–17113, 2017.
- [10] A. Kiani, B. R. Sutherland, Y. Kim, O. Ouellette, L. Levina, G. Walters, C. T. Dinh, M. Liu, O. Voznyy, X. Lan, A. J. Labelle, A. H. Ip, A. Proppe, G. H. Ahmed, O. F. Mohammed, S. Hoogland, E. H. Sargent, "Single-step colloidal quantum dot films for infrared solar harvesting," *Applied Physics Letters*, Vol. **109**, No. **18**, pp. 1-5, 2016.
- [11] W.M.M. Lina, M. Yarema, M. Liu, E. Sargentb, and V. Wood, "Nanocrystal Quantum Dot Devices: How the Lead Sulfide (PbS) System Teaches Us the Importance of Surfaces", *Colloidal Nano Crystals*, Vol. **75**, pg. 398–413, 2021.
- [12] C. Rajashree, A. R. Balu and V. S. Nagarethinam. "Properties of Cd doped PbS thin films: doping concentration effect". *Surface Engineering*, Vol. **31**, No. **4**, Pg. 316 -321, 2015.
- [13] M. M. Abbas, A. Ab-M. Shehab, A. K. Al-Samuraee, N. A. Hassan, "Effect of Deposition Time on the Optical Characteristics of Chemically Deposited Nanostructure PbS Thin Films," *Energy Procedia*, Vol. **6**, pp. 241–250, 2011.
- [14] K.C. Preetha, K. Deepa, A.C. Dhanya, T.L.Remadevi, "Role of complexing agents on chemicalbath deposited PbS thin film characterization," *Materials Science and Engineering*. Vol. **73**, pp. 1-5, 2015.
- [15] I. Dobryden, B. Touati, A. Gassoumi, A. Vomiero, N. Kamoun, N. Almqvist, "Morphological and electrical characterization of Cu-doped PbS thin films with AFM", *Advanced Materials Letters*, Vol. **8**, No. **11**, pp. 1029-1037, 2017.
- [16] L. N. Maskava, E. V. Mostovshchikova, V. I. Voronin, A. V. Pozdin, I. O. Selyanin, I. A. Anokhina, and V. F. Markov, "Structural and Electrical Properties of PbS Films Doped with Cr³⁺ Ions during Chemical Deposition", *Semiconductor*, Vol. **55**, No. **10**, pp. 937–946, 2021.
- [17] A.N. Nwori, L.N. Ezenwaka, E. I. Otti, N. A. Okereke, N. L. Okoli, "Study of the Optical, Electrical, Structural and Morphological Properties of Electrodeposited Lead Manganese Sulphide (PbMnS) Thin Film Semiconductors for Possible Device Applications", *Journal of modern materials*, Vol. **8**, No. **1**, pp. 40-51, 2021.
- [18] A. J. Yost, A. Pimachev; G. Rimal, J. Tang, Y. Dahnovsky; T. Y. Chien, "Effects of Mn dopant locations on the electronic bandgap of PbS quantum dots", *Applied physics Letters*, Vol. **111**, pp. 1-5, 2017.
- [19] A.N. Nwori, L.N. Ezenwaka, I.E. Otth, N.A. Okereke, N.S. Umeokwona, N.L. Okoli, I. O. Obimma, "Effect of Deposition Voltage Variation on the Optical Properties of PbMnS Thin Films Deposited by Electrodeposition Method", *Journal of Physics and Chemistry of Materials*, Vol.8, No. **3**, pp.12-22, 2021.
- [20] M. Shkir, M.T. Khan, I.M. Ashraf, S. AlFaify, A.M. El-Toni, A. Aldalbahi, ... A. Khan, "Rapid microwave-assisted synthesis of Ag-doped PbS nanoparticles for optoelectronic applications," *Ceramics International*, Vol. **45**, No. **17**, pp. 21975-21985, 2019.
- [21] S. Nazir, J.M. Zhang, M.N. Akhtar, N. Abbas, S. Saleem, M. Nauman, A. Ali, "Modification of physicochemical and electrical characteristics of lead sulfide (PbS) nanoparticles (NPs) by manganese (Mn) doping for electronic device and applications," *Journal of Sol-Gel Science and Technology*, Vol. **108**, No. **3**, 778-790, 2023
- [22] A.M. Ahmed, M. Rabia, M. Shaban, "The structure and photoelectrochemical activity of Cr-doped PbS thin films grown by

- chemical bath deposition,” *RSC advances*, Vol. **10**, No. **24**, pp. **14458-14470**, 2020.
- [23] Y. Gülen, “Characteristics of Ba-doped PbS thin films prepared by the SILAR method,” *Acta Physica Polonica A*, Vol. **126**, No. **3**, pp. **763-767**, 2014.
- [24] S.R. Rosario, I. Kulandaisamy, K.D.A. Kumar, A.M.S. Arulanantham, S. Valanarasu, M.A. Youssef, N.S. Awwad, “Deposition of p-type Al doped PbS thin films for heterostructure solar cell device using feasible nebulizer spray pyrolysis technique” *Physica B: Condensed Matter*, Vol. **575**, pp. **411704**, 2019.
- [25] I.M. Momoh, O.J. Akinribide, J.A. Olowonubi, J.O. Ayanleke, G.E. Olorunfemi, S.N. Echenim, A.E. Akin-Ponnle, “Effect of walnut shell powder on the mechanical properties of case-hardened steel,” *International Journal of Development and Sustainability*, Vol. **4** No. **2**, pp. **209-218**, 2015.
- [26] A.N. Nwori, L.N. Ezenwaka, I.E. Ottih, N.A. Okereke, N.L. Okoli, “Study of the Optical, Structural and Morphological Properties of Electrodeposited Copper Manganese Sulfide (CuMnS) Thin Films for Possible Device Applications,” *Trends in Sciences*, Vol. **19**, No. **17**, pp. **5747-5747**, 2022.
- [27] I. Afşin Kariper, S. Özden, F.M. Tezel, “Optical properties of selenium sulfide thin film produced via chemical dropping method,” *Optical and Quantum Electronics*, Vol. **50**, pp. **1-7**, 2018
- [28] L.N. Ezenwaka, A.N. Nwori, I.E. Ottih, N.A. Okereke, N.L. Okoli, “Investigation of the Optical, Structural and Compositional Properties of Electrodeposited Lead Manganese Sulfide (PbMnS) Thin Films for Possible Device Applications,” *Nanoarchitectonics*, pp. **18-32**, 2022.
- [29] A. Ohwofosirai, M.D. Femi, A.N. Nwokike, O.J. Toluchi, R.U. Osuji, B. A. Ezekoye, “A study of the optical conductivity, extinction coefficient and dielectric function of CdO by successive ionic layer adsorption and reaction (SILAR) techniques,” *American Chemical Science Journal*, Vol. **4**, No. **6**, pp. **736-744**, 2014.
- [30] I.L. Ikhioya, S. Ehika, N.N. Omehe, “Electrochemical deposition of lead sulphide (PbS) thin films deposited on zinc plate substrate,” *Journal of Materials Science Research and Reviews*, Vol. **1**, No. **3**, pp. **1-11**, 2018.
- [31] N.L. Okoli, L.N. Ezenwaka, N.A. Okereke, I.A. Ezenwa, A.N. Nwori, “Investigation of Optical, Structural, Morphological and Electrical Properties of Electrodeposited Cobalt Doped Copper Selenide (Cu_(1-x)Co_xSe) Thin Films,” *Trends in Sciences*, Vol. **19**, No. **6**, pp. **5686-5686**, 2022.
- [32] T. Chanthong, W. Intaratat, T.N. Wichean, “Effect of Thickness on Electrical and Optical Properties of ZnO: Al Films,” *Trends in Sciences*, Vol. **20**, No. **3**, pp. **6372-6372**, 2023.
- [33] M.I. Khan, S. Hussain, M. Fatima, S. Bano, M.S. Hasan, I. Bashir, M. Ammami, “Improved SnS: Mg thin film solar cells achieved by reduced recombination rate,” *Inorganic Chemistry Communications*, Vol. **157**, pp. **111361**, 2023.
- [34] M. Rajasekaran, A. Arunachalam, P. Kumaresan, “Structural, morphological and optical characterization of Ti-doped ZnO nanorod thin film synthesized by spray pyrolysis technique,” *Materials Research Express*, vol **7**, pp. **1-17**, 2020.
- [35] P.Gareso, H. Heryanto, E. Juarlin, P. Taba, “Effect of Annealing on the Structural and Optical Properties of ZnO/ITO and AZO/ITO Thin Films Prepared by Sol-Gel Spin Coating,” *Trends in Sciences*, Vol. **20**, No. **3**, pp. **6521-6521**, 2023
- [36] U.V. Okpala, F.I. Ezema, O.U. Rose, “Synthesis and Characterization of Local Impurities Doped Stannous Iodide (SnI₂) Crystal in Silica Gel,” *Advances in Applied Science Research*, Vol. **3**, No. **2**, pp. **1175-1184**, 2012.
- [37] U.V. Okpala, F.I. Ezema, O.U. Rose, “A study of the optical properties of un-doped and potash doped lead chloride crystal in silica gel,” *Advances in Applied Science Research*, Vol. **3**, No. **1**, pp. **103-109**, 2012.

AUTHORS' PROFILE

Achilefu Blessing Chinyere, completed her Bachelor of Science (B. Sc.) Degree under the close guidance of Professor U.V Okpala in the Department of Industrial Physics Chukwuemeka Odumegwu Ojukwu University Uli, Anambra State Nigeria in 2023. She has participated in quite numbers of local conferences within the University community prior to her graduation. She has a kin interest in the study of Nano-thin film semiconductors for solar energy applications and device applications.



Okpala Uchechukwu Vincent, earned his B. Sc degree in Physics in 1999 from the University of Calabar, Cross-River State, Nigeria, M. Tech. Physics electronics in 2005, from the Nnamdi Azikiwe University Awka Anambra State, Nigeria and Ph.D. in Solar energy Physics from University of Nigeria, Nsukka, Enugu State, Nigeria in 2012. He is a Professor with the Department of Industrial Physics, Chukwuemeka Odumegwu Ojukwu University, Anambra State, Nigeria. He is a member of Nigerian Institute of Physics (NIP), Member Solar Energy Society of Nigeria (MSESN) and Fellow Material Science Society of Nigeria (FMSN) and has published about 47 research papers both in international and local journals. He has 17 years of teaching experience. His areas of research interest are Solar energy Physics, Solid state Physics, Materials Science, Physics Environmental management and sustainability.



Nwori Augustine Nwode, obtained his Bachelor of Science (B. Sc.) Degree from Ebonyi State University Abakaliki, Ebonyi State, Nigeria, in 2009 and Masters of Science (M. Sc.) and PhD Degrees from Chukwuemeka Odumegwu Ojukwu University Uli, Anambra State, Nigeria in 2017 and 2021 respectively. He is a kin researcher in solid-state/solar energy physics with the Department of Industrial Physics Chukwuemeka Odumegwu Ojukwu University Uli, Anambra State, Nigeria. He has published about 17 research papers in reputable international and local journals. His main research interest focuses on the fabrications of new thin film materials for solar energy device applications and development.

